Letter of Intent for the SPSC Neutrino Platform Call

The ENUBET Project

F. Acerbi[a], G. Ballerini[b,o] M. Bonesini[b], C. Brizzolari[b,o], G. Brunetti[j] M. Calviani[m], S. Carturan[j,k], M.G. Catanesi[l], S. Cecchini[c], F. Cindolo[c], G. Collazuol[j,k], E. Conti[j] F. Dal Corso[j], G. De Rosa[p,q], C. Delogu[b,h], A. Falcone[j,k], B. Goddard[m], A. Gola[a], R.A. Intonti[l], C. Jollet[d], V. Kain[m], B. Klicek[s], Y. Kudenko[r], M. Laveder[j], A. Longhin[j,k(*)], P.F. Loverre[n,f], L. Ludovici[f], L. Magaletti[l], G. Mandrioli[c], A. Margotti[c], V. Mascagna[b,o], N. Mauri[c], A. Meregaglia[d], M. Mezzetto[j], M. Nessi[m], A. Paoloni[e], M. Pari[j,k,m], E. Parozzi[b,h], L. Pasqualini[c,g], G. Paternoster[a], L. Patrizii[c], C. Piemonte[a], M. Pozzato[c], F. Pupilli[j], M. Prest[o,b], E. Radicioni[l], C. Riccio[p,q], A.C. Ruggeri[p,q], G. Sirri[c], M. Soldani[o,b], M. Stipcevic[s], M. Tenti[b,h], F. Terranova[b,h], M. Torti[b,h], E. Vallazza[i], F. Velotti[m], M. Vesco[k], L. Votano[e]

[a] Fondazione Bruno Kessler (FBK) and INFN TIFPA, Trento, Italy
[b] INFN, Sezione di Milano-Bicocca, Piazza della Scienza 3, Milano, Italy
[c] INFN, Sezione di Bologna, viale Berti-Pichat 6/2, Bologna, Italy
[d] CENBG, Universite de Bordeaux, CNRS/IN2P3, 33175 Gradignan, France
[e] INFN, Laboratori Nazionali di Frascati, via Fermi 40, Frascati (Rome), Italy
[f] INFN, Sezione di Roma 1, piazzale A. Moro 2, Rome, Italy
[g] Phys. Dep. Università di Bologna, viale Berti-Pichat 6/2, Bologna, Italy
[h] Phys. Dep. Università di Milano-Bicocca, Piazza della scienza 3, Milano, Italy
[i] INFN Sezione di Trieste, via Valerio, 2 - Trieste, Italy
[j] INFN Sezione di Padova, via Marzolo, 8 - Padova, Italy
[k] Phys. Dep. Università di Padova, via Marzolo, 8 - Padova, Italy
[l] INFN Sezione di Bari, via Amendola, 173 - Bari, Italy
[m] CERN, Geneva, Switzerland
[n] Phys. Dep. Università La Sapienza, piazzale A. Moro 2, Rome, Italy.
[o] DISAT, Università degli Studi dell'Insubria, via Valeggio 11, Como, Italy
[p] INFN, Sezione di Napoli, Via Cintia, Napoli, Italy
[q] Phys. Dep., Universitá "Federico II" di Napoli, Napoli, Italy
[r] Institute of Nuclear Research of the Russian Academy of Science, Moscow, Russia
[s] Center of Excellence for Advanced Materials and Sensing Devices, Ruder Boskovic Institute, HR-10000 Zagreb, Croatia
[(*)] Contactperson

CERN-SPSC-2018-034 / SPSC-I-248
05/11/2018

Abstract

The knowledge of the initial flux in conventional neutrino beams represents the main limitation for a precision (1%) measurement of ν_e and ν_μ cross sections.

Since 2016, ENUBET has achieved remarkable results in the design of a neutrino beam with superior control of the fluxes and has extended its physics case to cover all the needs of new generation cross section experiments. In this Proposal, we summarize the achievement of ENUBET in the design and simulation of the proton extraction scheme, focusing system, transfer line and instrumentation of the decay tunnel. We present the results on positron reconstruction from the K_{e3} decays and the impact on the determination of the flux, outlining the activities that will be carried on during LS2 and the final validation of the ENUBET demonstrator in 2021. Special emphasis will be given on the activities that will be performed in collaboration with the CERN groups and the use of CERN facilities and infrastructures. In the Proposal, we also discuss the potential of monitored neutrino beams beyond the original aim of ENUBET: the flux measurement at the 1% level for all ν_μ produced in the beam and the determination of the neutrino energy without relying on final state particle reconstruction. In addition, the ENUBET static focusing system paves the way to the construction of a tagged neutrino beam, i.e. a facility where the observation of the lepton in the decay tunnel is associated with the neutrino scattering in the neutrino detector on an event-by-event basis. Perspectives and opportunities offered by tagged neutrino beams are discussed, too.

1 Introduction

Over the last 50 years, accelerator neutrino beams [1] have been developed toward higher and higher intensities but uncertainties in the flux and flavor composition are still very large. Thanks to the enormous progress in neutrino scattering experiments [2, 3], the measurements of neutrino cross sections are now limited by the knowledge of the initial fluxes, since the yield of ν_μ is not measured in a direct manner but relies on extrapolation from hadro-production data and a detailed simulation of the neutrino beamline. This limitation bounds the precision that can be reached in the measurement of the absolute cross sections to $\mathcal{O}(5-10\%)$. Moreover, pion-based sources mainly produce ν_μ while most of the next generation oscillation experiments will rely on the appearance of ν_e at the far detector. A direct measurement of the ν_e cross sections is, hence, of great interest for the current (T2K, NOvA) and next (DUNE, HyperK) generation of oscillation experiment [4]. These considerations motivated the development of "monitored neutrino beams" [5] and, in turn, the ENUBET proposal [6]: a facility where the only source of electron neutrino is the three body semileptonic decay of the kaons: $K^+ \to \pi^0 e^+ \nu_e$ (K_{e3}). In ENUBET, the electron neutrino flux is monitored in a direct manner by the observation of large-angle positrons in the decay tunnel.

The ERC ENUBET ("Enhanced NeUtrino BEams from kaon Tagging") project [7] is aimed to build a detector that identifies positrons in K_{e3} decays while operating in the harsh environment of a conventional neutrino beam decay tunnel. The project addresses all accelerator challenges of monitored neutrino beams: the proton extraction scheme (Sec. 3), focusing and transfer line (Sec. 4), instrumentation of the decay tunnel (Sec. 5 and 6) and the assessment of the physics performance (Sec. 7). The project has been approved by the European Research Council (ERC Consolidator, PI A. Longhin, Host Institution INFN, Grant Agreement 681647) for a five year duration and a 2.0 M€ budget. ENUBET started on 1 June 2016 and by now the ENUBET Collaboration consists of 58 physicists from 12 institutions.

In the following, we summarize the results achieved after two years and outline the activities during and after LS2. We review also the potential of monitored neutrino beams as source of virtually monochromatic beams (Sec. 7): due to the narrow momentum bite of the ENUBET extraction line, the neutrino energy of each event is known from the position of the interaction vertex with a precision ranging from 7% to 22% over a broad momentum range (0.8-3.5 GeV). Finally, we review the additional advantages of a purely static focusing system, which is one of the most remarkable achievement of the ENUBET R&D in 2016-2018. A static system coupled with a narrow band extraction line allows for the monitoring of the ν_μ from pion decays and paves the way to tagged neutrino beams (Sec. 8).

This Letter of Intent updates the Expression of Interest submitted to the SPSC in October 2016 [6] and reviews the activities that the ENUBET Collaboration is planning at CERN and the requests for the use of CERN facilities and infrastructures.

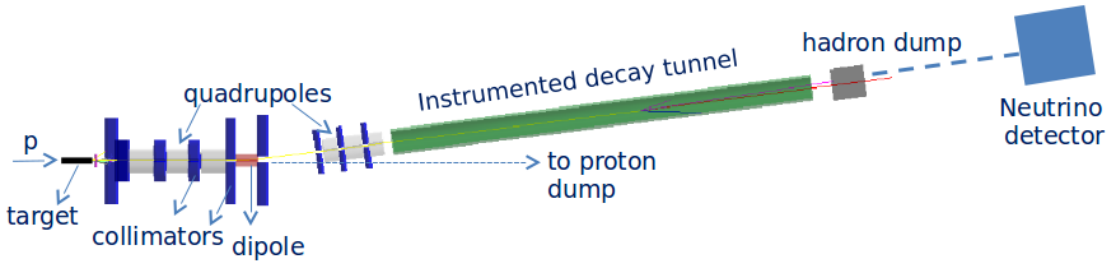

Figure 1: Schematics of the ENUBET neutrino beam in the static focusing option (not to scale).

2 An overview of ENUBET neutrino beam

The ENUBET neutrino beam is a conventional narrow band beam with a short (∼20 m) transfer line followed by a 40 m long decay tunnel. Unlike most of the beams currently in operation, the decay tunnel is not located in front of the focusing system (horns) and the proton extraction length is slow: a few ms in the horn option and 2 s in the static focusing option (see Sec.4). Particles produced by the interaction of protons on the target are focused, momentum selected and transported at the entrance of the tunnel. Non-interacting protons are stopped on a proton beam dump.

The particles that reach the decay tunnel are hence pions, kaons and protons within the momentum bite of the transfer line (10% in ENUBET). Off-momentum particles are mostly low energy pions, electron, positron and photons from tertiary interactions in the collimators and other components of the beamline, and muons from pion decay that cross the collimators. The rate of these particles are several orders of magnitude smaller than beams currently in operation and particle creation in the decay tunnel can be monitored at single particle level by instrumenting a fraction of the decay tunnel.

Kaon decays are particularly well suited for single-particle monitoring. In ENUBET the mean energy of the hadrons selected in the transfer line (8.5 GeV) and the length of the decay tunnel is optimized in order to have only one source of electron neutrinos: the K_{e3} decay of the kaons - $K^+ \to \pi^0 e^+ \nu_e$. Electron neutrinos from the decay in flight of kaons represent $\sim$ 97% of the overall ν_e flux. Since the positrons are emitted at large angles with respect to muons from pion decay, particles produced by the kaons reach the wall of the instrumented tunnel before hitting the hadron dump (see Fig. 1). The vast majority of undecayed pions, particles transported along the transfer line and muons from $\pi^+ \to \mu^+ \nu_\mu$ reach the hadron dump without hitting the walls and do not contribute to the particle rate in the instrumented walls.

The rate of positrons from K_{e3} decays is monitored at single particle level by longitudinally segmented calorimeters that separate positrons from pions, muons, neutrons

and protons. The modules of the calorimeter are located inside the beam pipe and are assembled into cylindrical layers. Positron/photon separation is performed by a photon veto made of plastic scintillator tiles located just below the innermost layer.

The rate of positrons provides a direct measurement of the ν_e produced in the tunnel. The distribution of particles (positron, muons, pions) along the axis of the tunnel and their energy and polar angle distribution constrain any source of systematic bias between the rate of positrons observed in the tunnel and the expected rate of ν_e at the detector. Unlike present beams, at leading order no information is needed from particle production yields in the target (hadro-production), the simulation of transport and reinteraction of secondary particles in the beamline, the monitoring of the protons-on-target (pot) and of the currents in the horn because the rate of particle production in the tunnel provides an observable that is directly linked to the flux. ENUBET is now studying sub-leading effect to demonstrate that the total systematic budget of the ν_e flux is below 1%.

Since the K_{e3} branching ratio is known with a precision of 0.8%, positron monitoring also provides the total production rate of kaons at the per-cent level. This precision can be further improved monitoring the rate of pion production in the tunnel due to the other decay modes of kaons and, in particular, the leading $K^+ \to \mu^+\nu_\mu$ (BR $\simeq$63%) and $K^+ \to \pi^+\pi^0$ (BR $\simeq$21%). These channels, which were not included in the original physics programme of ENUBET, are now exploited to evaluate the flux of ν_μ from kaons. Finally, a direct measurement of the rate of muons from π^+ decays after the hadron dump cannot be done at single particle level for the horn-based option but it can be performed if the focusing is purely static because the muon rate is reduced by two order of magnitudes (see Sec. 4). In this case, the muon rate after the hadron dump provides the ν_μ flux from pion decays with a precision comparable with the ν_e flux.

ENUBET can be operated in inverse-polarity mode, producing $\bar{\nu}_e$ from $K^- \to \pi^0 e^- \bar{\nu}_e$ and $\bar{\nu}_\mu$ from $\pi^- \to \mu^- \nu_\mu$ and $K^- \to \pi^0 e^- \bar{\nu}_e$. All considerations above apply to ENUBET as a source of electron and muon antineutrinos.

3 Proton extraction schemes

Monitoring of the kaon decay product in the decay tunnel can be performed at single-particle level only if the duration of the proton extraction is slower than current long-baseline neutrino beams (tens of μs) in order to keep the particle rate in the decay tunnel at a sustainable level. The maximum length depends on the implementation of the focusing system for the secondary particles produced in the target. A horn-based system cannot be sourced in DC mode and the maximum current pulse duration is $\sim$10 ms. A static focusing system, however, can be operated in DC mode and proton extractions up to several seconds can be envisaged. ENUBET is pursuing both options and developing a dedicated proton extraction scheme both at the ms ("burst-mode

extraction") and the second ("slow extraction") scale.

The development of the proton extraction scheme at CERN-SPS is performed in collaboration with BE-OP-SPS and TE-ABT. The first goal of the project is to model and optimize the stability of the present slow extractions at the SPS, characterized by spill lengths of the order of 1 s. The second goal is to carry out a theoretical and experimental investigation into controlling the burst-mode slow extraction. This burst extraction scheme has been conceived in [6] in the framework of ENUBET. It has, however, potential applications beyond neutrino physics because it allows to increase by more than one order of magnitude the maximum particle rate to beam users within a cycle of fixed length, extracting a constant number of protons per cycle.

The burst mode consists of extracting many consecutive spills (duration: a few ms) within one macro SPS spill (duration: ∼4 s). This scheme allows to employ magnetic horns in the ENUBET transfer line (see Sec. 4).
We are currently implementing the extraction scheme in the SPS in a proof-of-concept version and testing it before LS2. The optimization of the machine parameters will be based on the outcome of the current measurement campaign and will be validated after LS2.

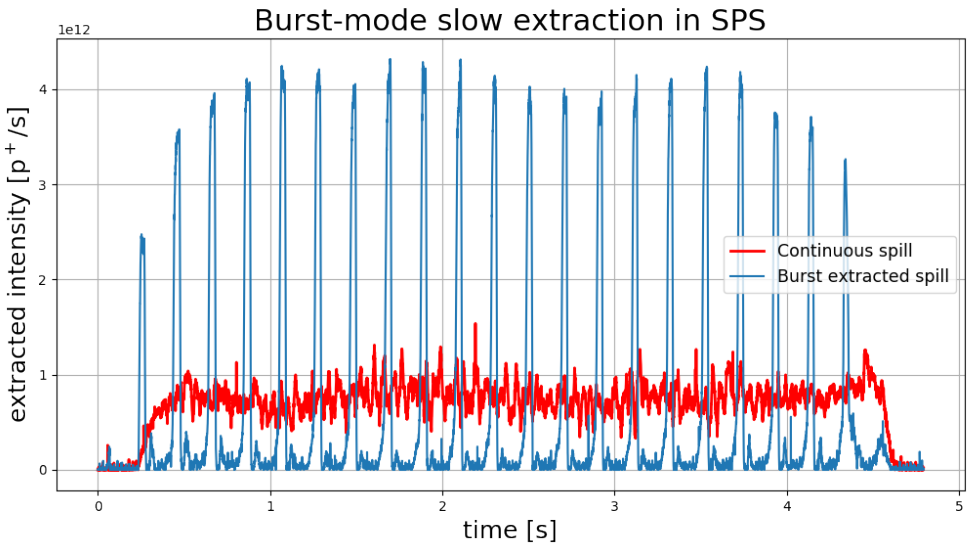

Figure 2: Continuous spill (red) as currently extracted to the North Area and burst-mode slow extraction spill (blue). Data were collected during the SPS machine development in summer 2018.

Fig. 2 shows the first results of the 2018 campaign, where the burst extraction scheme has been implemented on the 4.8 s-long spill of the SFTPRO cycle. Burst-mode is enabled acting on the tune of the machine and exploiting the quadrupole-driven slow extraction at the SPS. Early results from 2018 indicate that:

- This proton extraction scheme successfully extracts all the circulating protons per cycle. Concerning machine efficiency, the dumped intensity per cycle does not increase with respect to the present continuous operation ($\simeq 3\%$ of the circulating intensity) with spill lengths between 9 and 20 ms at a repetition rates of 10 Hz.

- Setting the burst-mode slow extraction in operation takes only one change of parameter of the LHC Software Architecture (LSA). We proved that it is possible to switch on and off the burst extraction even inside the same SPS cycle.

- The intensity of each spill can be adjusted up to the nominal ENUBET intensity. For instance, for a 10 ms spill, the maximum pot per second that could theoretically be achieved are higher than 9×10^{13}.

Regarding the spill quality, the effective spill length parameter defined in [8] showed a degradation when going from a spill length of 20 ms (spill in good agreement with a square wave) to a spill length of 9 ms. The effect of different machine components (e.g. sextupoles), will be investigated to recover such a degradation.
Moreover, the optimization of the machine parameters can be performed empirically using the measured extracted intensity in a feed forward fashion, optimizing towards a reference spill structure [9]. The burst extraction has been successfully implemented for a feed forward optimization scheme and it is currently under test at the SPS.

4 Focusing and transfer line

The optimization of the ENUBET transfer line proceeds toward three steps. First, the optics of the transfer line is simulated with TRANSPORT [10] and optimized to match the ENUBET specifications for momentum bite and beam envelope.

The beam component and lattice are then implemented in G4Beamline [11] that fully simulates particle transport and interactions. There are several possible configurations in terms of elements (quadrupoles and dipoles) that can be used to transport K^+ and π^+ to the instrumented decay tunnel. The optimization is performed with regards to:

- the number of K^+ and π^+ in the momentum range of interest for ENUBET at the entrance of the decay tunnel

- the total length of the transfer line, which has to be minimized to reduce kaon decay losses before the entrance of the decay tunnel

- the beam size and envelope since non-decaying particles must exit the decay tunnel without hitting the tunnel walls

- the field and aperture of the magnets, which should enable the use of normal-conducting, conventional devices

- the level of background transported to the tagger, which affects signal-to-noise (S/N) of identified positrons (see Sec.6)

In the static focusing system quadrupoles are placed directly downstream the ENUBET target while the horn-based design needs a focusing magnetic horn between the target and the quadrupoles. In this document we describe more in detail the static design, whose performance turned out to be significantly better than early estimates reported in the ENUBET proposal [5] and it offers several advantages in terms of cost, simplification of technical implementation and performance of particle identification (see below). Results obtained for the horn-based transfer line are presented as well for comparison and horn-based studies will also be pursued due to the remarkable ν fluxes that can be achieved.

Primary proton interactions in the target are simulated with FLUKA 2011. The target considered is a 1 m long Beryllium cylinder. This target is being replaced by a Graphite target, which eases substantially the thermo-mechanical design and provide similar yields as the Be target and negligible secondary interaction effects. The results presented here are based on the SPS as proton driver (400 GeV protons) but other existing proton drivers have been considered as well (120 GeV and 30 GeV protons).

The reference TRANSPORT beam for the optic optimization has a central momentum of 8.5 GeV/c with a momentum bite of 10%. The best configuration achieved consists of a quadrupole triplet followed by a bending dipole followed by another quadrupole triplet. The dipole and all the quadrupoles have an aperture radius of 15 cm. The dipole field is 1.8 T providing a bending angle of 7.4°. Fields at pole in the quadrupoles are in the range 5-11 kG. This configuration has been implemented in G4Beamline with the addition of absorber between elements, a Tungsten foil after the target to screen positrons that would otherwise reach the tagger and a low power hadron dump at the end of the decay tunnel (see Fig. 1).

In the present beamline design, absorbers are made of iron blocks to stop beam particles and shield the magnets. The re-optimization of the collimators in terms of size and material choice is underway in collaboration with CERN A&T. The dose assessment is being performed with FLUKA. A proton dump will stop primary protons that have not interacted in the target. It will be placed on-axis with respect to the incident proton beam, its exact position, material composition and dimensions are under study.

Particle yields at the tagger entrance from $\sim 4 \times 10^6$ simulated pot are summarized in Tab. 4 [12, 13]. Fig. 3 shows the momentum distribution for K^+ at the tagger entrance and exit. About 50% of K^+ decay in the 40 m long tunnel. The momentum spectrum at the tunnel exit is affected by the kaon loss due to the decays as well as minor losses due to interactions in the tunnel walls.

As noted above, the kaon yield in the static focusing system is four times larger than the original ENUBET proposal [5] due to the re-optimization of the beam optics. On the other hand, the horn based option still retains the highest yield (useful mesons per proton-on-target).

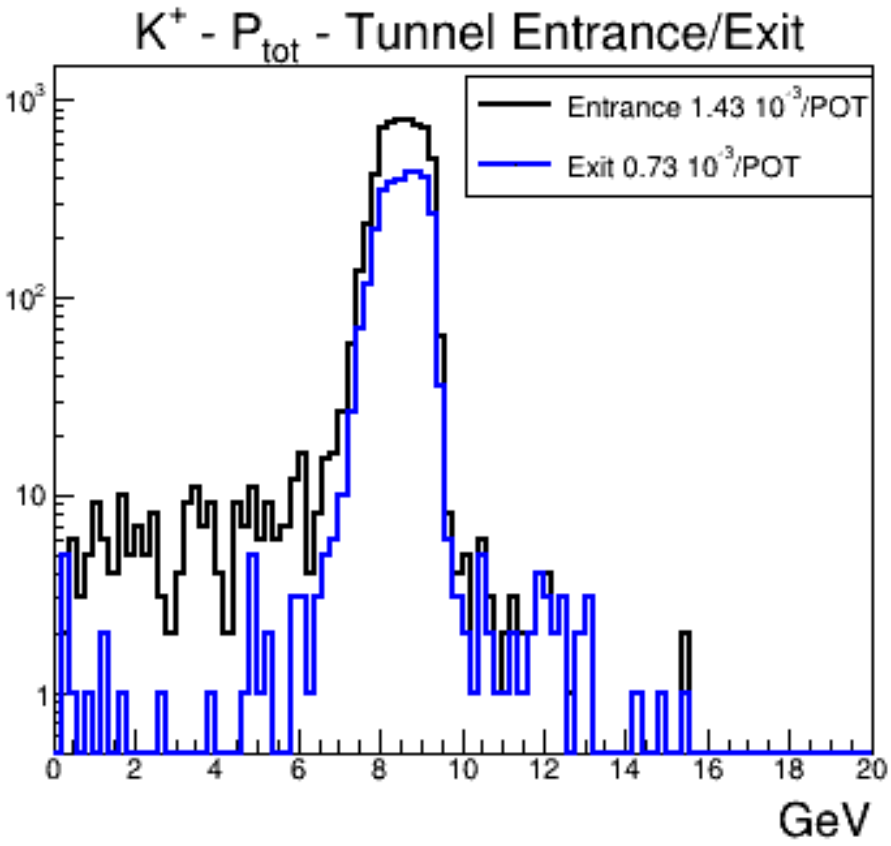

Figure 3: Momentum distribution obtained with G4beamline for K^+ at the tagger entrance and exit.

Focusing	π^+/pot $[10^{-3}]$	K^+/pot $[10^{-3}]$	Extraction Length	π/cycle (10^{10})	K/cycle (10^{10})	Factor w.r.t. [5]
Horn-based	77	7.9	2 ms	347	36	$\times 2$
Static	19	1.4	2 s	86	6.3	$\times 4$

Table 1: Expected rates of π^+ and K^+ in [6.5÷10.5 GeV] range at the decay tunnel entrance for the two possible focusing schemes. The improvement factor in kaon transport with respect to Ref. [5] is shown in the last column.

5 Instrumentation of the decay tunnel

The ENUBET instrumented decay tunnel consists of a calorimeter for e^+/π^+ separation and of an inner light-weight detector for e^+/π^0 separation and timing (t_0-layer).

5.1 The calorimetric section

Fast calorimeters with longitudinal segmentation are the preferred option for identifying positrons of a few GeV energy in the ENUBET instrumented decay tunnel. The baseline option is based on plastic scintillators that offer an energy resolution appropriate for the needs of ENUBET, short recovery time ($\sim$ 10 ns) and reduced costs. The calorimeter is built upon a basic unit (UCM, Ultra Compact Module) consisting of a stack of steel tiles (1.5 cm thick) interleaved with plastic scintillator tiles (0.5 cm thick) both having a 3×3 cm^2 cross section. As a result of an optimization based on the studies of the reconstruction Work Package (WP5 - see Sec. 6) the detector (see Fig. 4, left) consists of three layers of UCM in the radial direction for a total thickness of 9 cm. The inner radius of the tagger and its extension including longitudinal and azimuthal coverage are being studied including information from the reconstruction algorithms and the design of the hadronic beamline. A radius of 1 m allows to mitigate pile up due to stray particles in the beam halo and reduces detector irradiation. Future improvements of the hadronic beamline will likely allow to decrease the inner radius and to increase the geometrical efficiency of the tagger.

Appropriate e^+/π^+ separation is achieved using the pattern of the energy deposition in each UCM. Positron-initiated e.m. showers are fully contained inside ~ 2 UCM while pion-induced showers are more penetrating. The UCM axis is parallel to the beam because most of the particles impinges on the calorimeter with an angle below 100 mrad. The use of these calorimeters in a neutrino decay tunnel required a dedicated optimization with respect to standard applications at colliders where particles originate from a fixed interaction point.

We have considered and tested two possible schemes for light readout:

- **compact "shashlik"** readout (Fig. 4). In this configuration wavelength shifting (WLS) fibers run perpendicular to the tiles in a matrix of holes. Each module hosts nine 1 mm diameter fast WLS fibers with a decay time of < 3 ns and a density of about 1 fiber/cm^2. Fibers are readout individually by a SiPM positioned

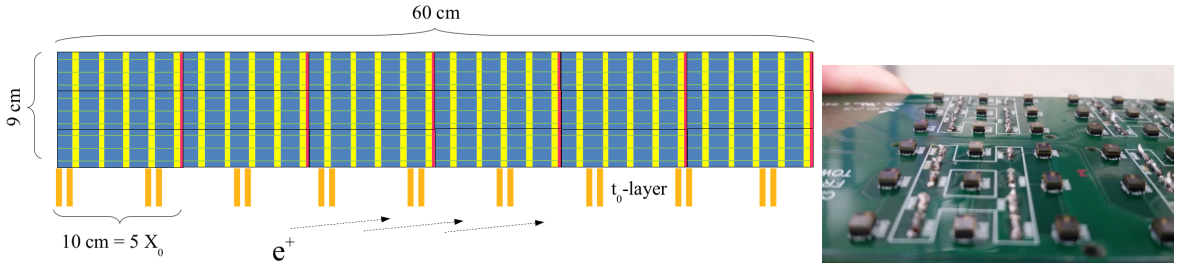

Figure 4: Left: A scheme of a tagger module in shashlik mode. Steel absorbers are shown in blue, scintillators in yellow and WLS fibers in green. The red boxes represent the PCBs with embedded SiPM. Right: a picture of a PCB hosting the SiPMs that has been developed for ENUBET.

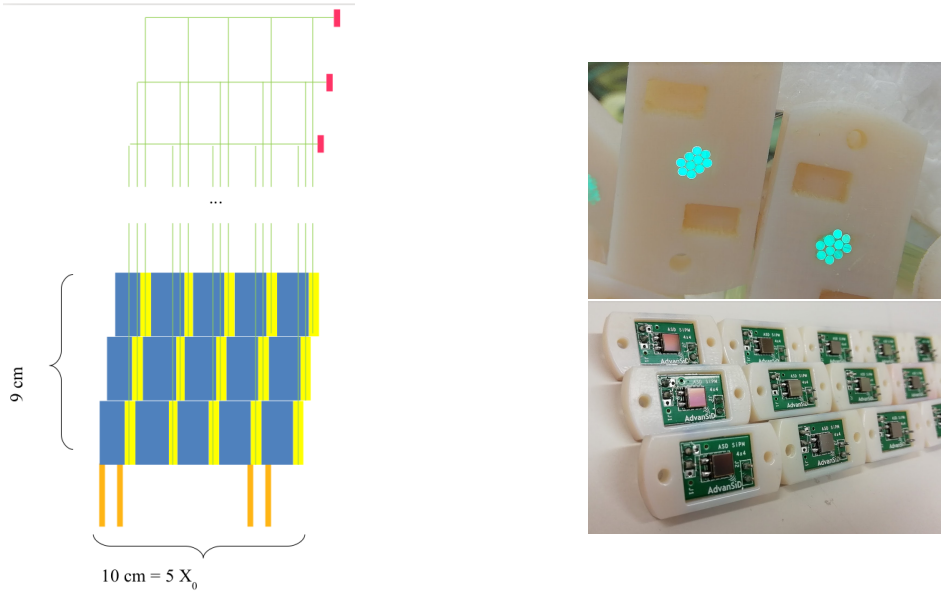

Figure 5: Left: A scheme of a tagger module in lateral readout mode made of steel absorbers (blue), scintillators (yellow) and WLS fibers (green). The red boxes represent the PCBs with embedded SiPM. Right: pictures of a UCM fiber bundle and connector (top) and 4×4 mm^2 SiPM.

at the back of the module. The photon readout layer encloses 9 SiPM (1 mm^2 active surface, cell size < 30 μm) encapsulated in a PCB and a plastic mask that links the fibers to the active area of the SiPM (Fig. 4, right). Benefiting from the compactness and high quantum efficiency of SiPM [14, 15, 16] and coupling these devices directly to individual fibers we achieve an homogeneous longitudinal sampling avoiding non-uniformities in the active region introduced by fiber bundles. This solution provides very compact devices and is extremely elegant. On the other hand it requires to operate silicon-based devices in the calorimeter bulk, exposing them to a large neutron flux (10^{11} 1MeV-eq n/cm^2) originated mainly by the hadronic interactions of kaon decay products.

- **"Lateral"** readout. In this scheme, the light is readout at both sides of each scintillator tile by glueing the WLS fiber to the scintillator inside a suitable groove machined on the plastic. Fibres from the same UCM are bundled in groups of ten and coupled to a 4×4 mm^2 SiPM at a distance of about 40 cm from the bulk of the calorimeter. In this scheme (Fig. 5) the SiPM are located in a low radiation area and can be accessed for maintenance or replacement. Furthermore, the lateral scheme is mechanically simpler both from the point of view of machining of the calorimeter component and for the fiber-to-sipm coupling.

The signal is readout in triggerless mode by waveform digitizers that sample and record the summed output of the 9 SiPM in the shashlik scheme or the output of a single larger SiPM for lateral readout.

5.2 The t_0 layer

Photons originating from $K^+ \to \pi^+\pi^0$ ($K_{\pi 2}$) decays and reaching the positron tagger [5] must be discriminated from positrons by a suitable photon veto. This detector also provides coarse information on the impact point of the particle and timing information. In the baseline option for the t_0 layer the basic unit is a doublet of plastic scintillator tiles (T0 doublet) with a $\sim 3 \times 3$ cm^2 surface and a 0.5 cm thickness (~ 0.02 X_0), readout by a WLS fiber optically linked to a SiPM. The doublets are orthogonal to the tagger axis and mounted below the inner radius of the calorimeter (orange in Fig. 4, left). Adjacent tiles form a ring installed inside the positron tagger. Along the z-axis, t_0 layer rings are separated by 7 cm to have on average about five hit doublets for K_{e3} positrons. Photon conversions are discriminated from positrons using the information on the pulse height in all hit scintillators. Photon converted in the photon veto are rejected requiring a signal compatible with a single mip (1-2 mip separation).

5.3 Test beam campaign in the East Hall

The **CERN East Area** is an ideal infrastructure for ENUBET and it will maintain such a prominent role for the tests of the final demonstrator after LS2. Figure 6 (top left) shows a picture of the shashlik prototype tested in November 2016 to assess the

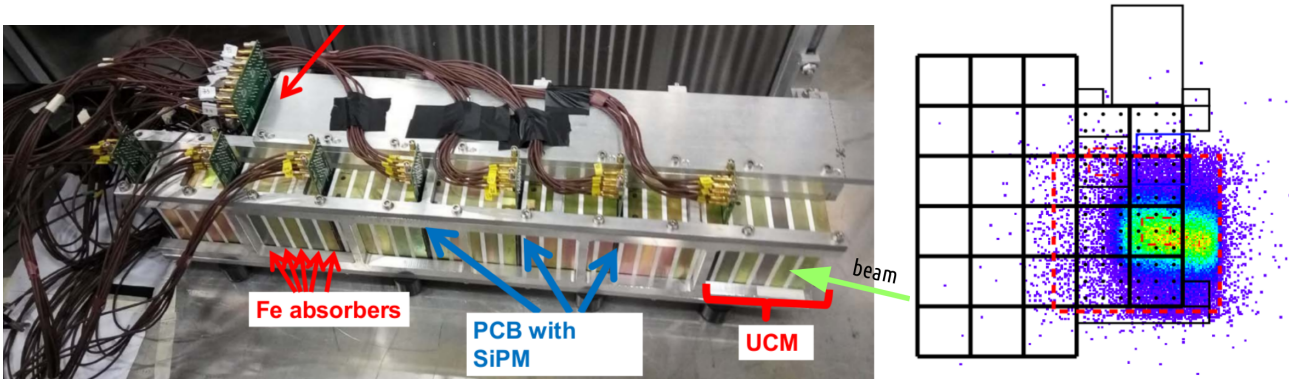

Figure 6: (Top Left): The prototype exposed at the CERN-PS T9 particle beams. The calorimeter is composed of an inner part (bottom part of the picture) made of seven calorimetric blocks and a 60 cm long "hadronic" block in the outer part (upper part of the picture). The system was mounted on a tunable mechanical cradle to record particles impinging at different angles. (Top Right): distribution of the tracks' impact parameters on the front side of the calorimeter as predicted from Silicon tracking chambers using the 5 GeV beam. The layout of the calorimeter is superimposed: each square represents a 3×3 cm^2 UCM. (Bottom): The lateral readout prototype tested at the PS-T9 area in September 2018. The t_0-layers are also visible in the bottom right part of the picture.

e/π discrimination capabilities with a pion containing setup. A prototype of the same size that provides good pion containment was tested in September 2018 using the lateral readout scheme (Fig. 6, bottom).

During 2016-2018 we performed tests in four two-week slots of data taking to val-

idate prototypes for the t_0-layer and the calorimeters both in shashlik and lateral readout modes. Using test beam data [17, 18] we have:

- established the effectiveness of both the shashlik layout enhanced by the longitudinal sampling and the lateral readout options
- measured the energy resolution for electrons and hadrons between 1 and 5 GeV and studied e^+/π^+ separation with a detailed characterization of lateral leakage and data/Monte Carlo validations
- determined the maximum particle rate that can be sustained by the tagger without compromising the particle identification performances
- gained inputs for tuning the detector granularity and reach the best cost-performance ratio. This optimization includes the size of the SiPM to prevent saturation, the number of SiPM to be summed and the parameters of the waveform digitizers
- characterized the response to particle beams of calorimeters equipped with neutron irradiated photosensors

In particular, we performed controlled irradiation tests of the SiPM employed in the Shashlik option using the CN accelerator at the INFN-LNL laboratories in June 2017 [19].
The ENUBET t_0 layer is based on a conventional technology and

- we developed the readout system based on a pair of lateral WLS fibers and custom amplifiers. The setup provides sufficient light yield and uniformity without compromising the material budget and cost-effectiveness.
- we validated with real data the 1-mip versus 2-mip separation capability and the background induced by lateral calorimeter leakage and albedo.

The results of the tests demonstrate that the shashlik option is appropriate for the needs of ENUBET. The testbeam data on the lateral scheme are under analysis. In 2019, the Collaboration will take the decision on the scheme to be used for the final demonstrator.

6 Particle reconstruction

Particle identification in the instrumented tunnel starts from an event seed associated to a large energy deposit. The first step needed for particle identification (PID) is the definition of the event by the ENUBET Event Builder (EB). Depending on the proton rate on the target and the recovery time of the UCM, several events will reach simultaneously the instrumented tunnel and pile-up effects are, in general, non negligible. An extensive work, based on a GEANT4 full simulation of the calorimeter, has been

carried out in order to mitigate pile up and reconstruct events to monitor positron production at single-particle-level. The PID algorithm analyses all the simulated events at the same time and merge the energy of the different UCMs if the occurrence of the energy deposit is within 1 ns. The algorithms developed in 2016-2017 were optimized for the observation of positron i.e. for a K_{e3} signal. Complementary analysis to extract a pure sample of two body muon decays $K_{\mu 2}$ and two body hadron decays $K_{\pi 2}$ are being investigated to gain additional information on the overall kaon rate and the flux of ν_μ from kaons.

In the standard positron identification analysis [20], all the UCMs of the first e.m. layer in which an energy deposition is found are ordered in time and the first available UCM with a visible energy larger than 20 MeV is selected as the *seed* of the event. Only UCMs/T0 doublets that are closest neighbors in ϕ to the seed in a time window of ± 1 ns with respect to the seed time are considered for the event building. Similarly, only UCMs with a longitudinal position in an interval of [-20,50] cm for e.m. layer, [-10,70] cm for hadronic layer (third upper layer) and T0 in [-30,0] cm with respect to the seed position are considered for the event building. If at the end of the loop over all the energy deposited we associate more than 9 UCM and the fraction of energy in the hadronic layer is below 20% the events is considered for the subsequent analysis. Then, all the associated UCMs and T0 doublets are discarded from the list of energy depositions and the process is repeated for a new event until all energy deposits are associated.

Once the event has been defined, particle reconstruction based on the excellent calorimetric capabilities of the detector as well as on the information coming from the T0 tagger can be carried out. Charged particles will deposit energy in different UCMs and the geometrical pattern of the energy deposition can be exploited to perform particle identification (PID). Indeed positrons will produce showers well contained in the first two electromagnetic layers and in few UCMs along the longitudinal coordinate, whereas pions will have a less compact shower and a larger fraction of energy deposited in the hadronic layer. To exploit as much as possible the calorimeter information we used a Neural Network (NN) based on TMVA multivariate analysis. In particular we used 11 variables such as the fraction of energy in the first e.m. layer, the fraction in the event seed and several other variables containing information on the shower profile development. The NN analysis allows to separate positrons from pions and muons but does not remove the contamination of photons from π^0 decays. The e^+/γ separation is performed using the signal of the T0 layer. Looking at the energy deposited in the two layers of the doublet we can discriminate between zero, one or two m.i.p. selecting positrons and rejecting photons converting in the first T0 layer. The T0 performance has been validated during a testbeam in October 2018.

Finally, two sequential cuts are applied that account for the positron density in space due to the finite dimension of the transfer line and the presence of the bending magnet. As shown in Fig. 7, positrons are mostly located in the downstream half of the tunnel, where contributions from large angle off momentum particles or products from particle interacting in the beam line components are reduced because they hit the upstream part

of the tunnel. Similarly, particles bent by the dipole and crossing the collimators are mostly located in the horizontal plane. Applying a two-dimensional cut in the visible energy versus distance along the tunnel plane and a cut on particles reconstructed in the horizontal plane, positrons are selected with a signal-to-noise ratio of ~ 0.5 and an efficiency of $\sim 20\%$, which is appropriate for the neutrino flux monitoring at the per-cent level. This level of reconstruction is achieved for the static focusing system assuming a complete extraction of the protons from the SPS lattice in a super-cycle (4.5×10^{13} pot in a 2 s slow extraction).

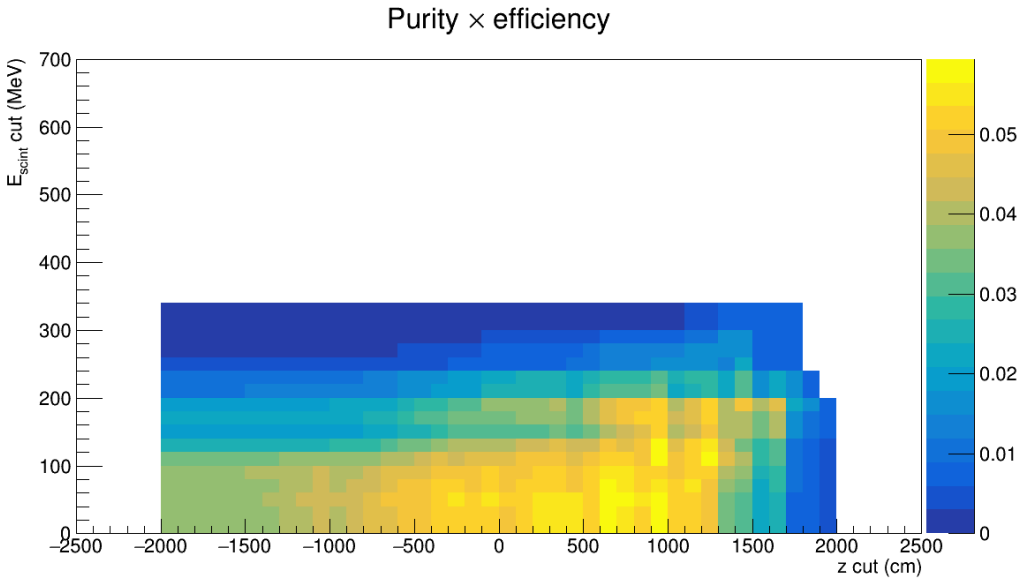

Figure 7: Purity×Efficiency achieved for the positron identification as a function of the cut on the total energy deposited in the scintillator (E_{scint}) and the position along the tunnel (z).

7 The ENUBET narrow band beam

ENUBET has been originally conceived as a facility to precisely measure the electron neutrino flux and perform a high precision ν_e cross section measurement. In fact, two additional features can be exploited to enhance the ENUBET physics programme. The narrow momentum width of the beam provides a precise measurement of the neutrino energy on event by event basis without relying on the reconstruction of final state particles. This is of paramount importance to measure the differential cross section without biases due to energy reconstruction (final state interactions, particle misidentification, detector effects). In addition, the slow extraction scheme reduces by two orders of magnitude the muon rate after the beam dump and allows for a high precision measurement of the ν_μ flux from π decays in addition to the ν_e and ν_μ flux

from kaon decay. These additional opportunities will be evaluated by the ENUBET Collaboration during LS2.

In order to assess the physics potential of the ENUBET narrow band beam in terms of expected neutrino interactions, a 500 ton liquid Argon detector (isoscalar target), placed 90 m from the entrance of the decay tunnel (50 m from the hadron dump) and with a cross-sectional area of 6×6 m^2 has been considered.

Neutrino fluxes were estimated simulating samples of positive pions and kaons with a momentum bite of 10% centered at 8.5 GeV/c. Corrections coming from neutrinos produced in the transfer line are now available from the end-to-end simulation of the beamline (see Sec. 4) and are being implemented in the full simulation. Decays of pions, kaons and of particles produced in their re-interactions with the tunnel instrumentation have been taken into account too. The assumed meson yields are the ones determined for the static transfer line described in section 4, considering 400 GeV protons, i.e. 19×10^{-3} π^+/pot and 1.4×10^{-3} K^+/pot. The interaction rates are the result of the convolution of the calculated fluxes at the detector with neutrino CC cross-sections. The detailed detector response is not included.

Assuming 4.5×10^{19} pot, about 1.13×10^6 ν_μ^{CC} and 1.4×10^4 ν_e^{CC} interactions will be observed at the neutrino detector. The current ENUBET beamline has been optimized for the energy range of interest for DUNE. The spectrum of ν_e^{CC} events, shown in Fig. 8, has a mean energy of 4 GeV and a FWHM of $\sim$3 GeV. A low energy running scheme optimized for the HyperKamiokande energy range is also under study.

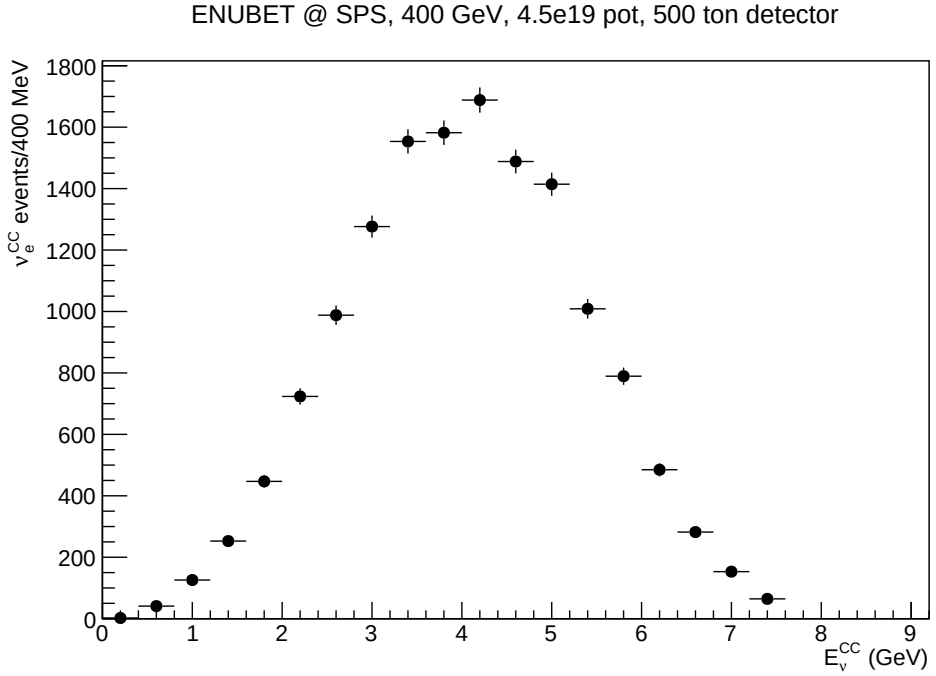

Figure 8: ν_e^{CC} interaction spectrum.

As mentioned above, ENUBET not only provides a beam with a precisely measured flux but also a measurement of the neutrino energy that does not rely on the reconstruction of final state particles. This feature ("narrow-band off-axis technique") results from the narrow momentum bandwidth of the beam and the finite transverse dimension of the neutrino detector, as long as detectors have a size comparable or larger than ICARUS at Fermilab or the Protodune's at CERN.

The energy measurement exploits the strong correlation between the energy of the neutrino interacting in the detector and the radial distance (R) of the interaction vertex from the beam axis (Fig. 9, left plot). By selecting interactions in radial windows of $\pm$10 cm at R equal to 0.5 m, 1.5 m and 2.5 m (Fig. 9, right plot), we collect samples of about 15.7×10^4, 6.4×10^4 and 2.9×10^4 ν_μ^{CC} events respectively. The pion component, in particular, covers well the energy range of interest for future long baseline oscillation experiments. The incoming neutrino energy is determined with a precision given by the pion peak width of the spectrum at a fixed R. It ranges from 7% at 3.5 GeV to 22% at 0.8 GeV, as illustrated in Fig. 10. Only a loose cut on the visible energy is needed to separate the ν_μ from pion decay from the ν_μ originating from the two body kaon decay. In this way, differential cross section measurements can be performed without relying on the reconstruction of the final state products for the determination of the neutrino energy. Absolute ν_μ cross section measurements can be performed combining the narrow-band off-axis technique with the measurement of the ν_μ flux from pion decay during the 2 s long extraction (static focusing scheme). The precision of flux measurement in a very slow extraction (2 s) can be performed at single particle level using radiation hard scintillators located after the beam dump. This technique, however, has not been demonstrated yet at the per cent level and its validation is one of the aim of ENUBET during LS2.

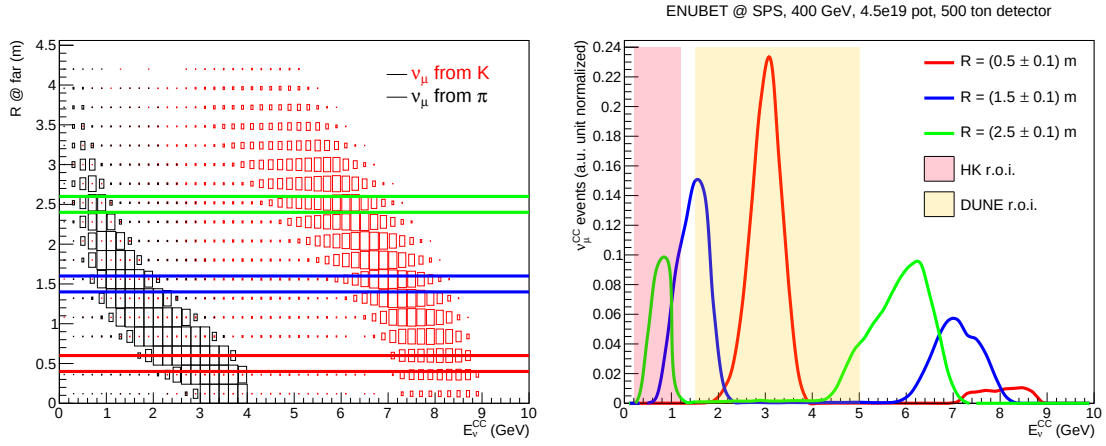

Figure 9: (Left) Radial and energy distribution of ν_μ^{CC} interactions. The high energy neutrino component from kaon decays is shown with red boxes, while the low energy one is reported with black boxes. (Right) ν_μ^{CC} spectra normalized to unity obtained selecting interactions at different radial distances from the beam axis.

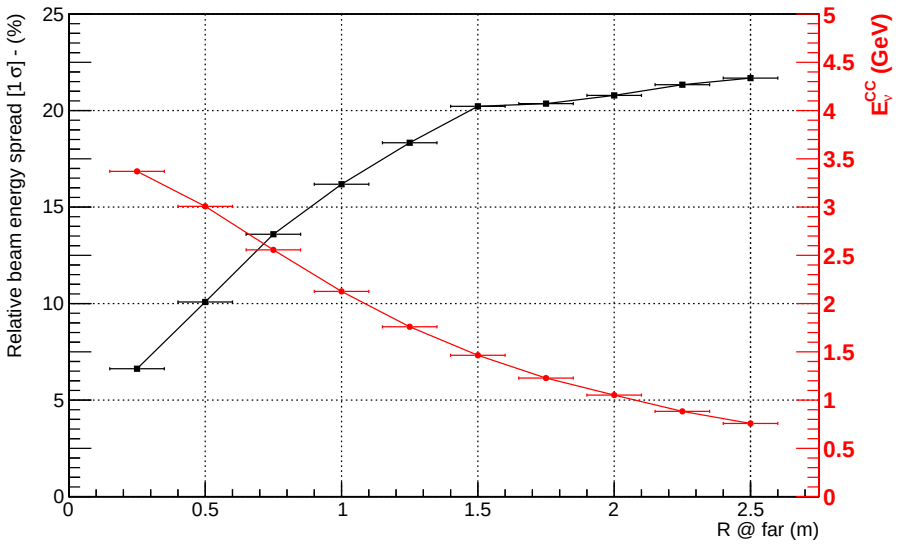

Figure 10: Beam energy spread (in black) and peak energy (in red) as a function of the distance R of the interaction vertex at the detector from the beam axis.

8 From monitored to tagged neutrino beams

A purely static focusing system opens up several opportunities beyond the original goals of ENUBET. Since the proton extraction can be diluted up to several seconds, the instantaneous rate of large angle decay products in the decay tunnel is reduced by about two orders of magnitude compared with the horn option. In the ENUBET static option the time between two K_{e3} decays is 1.3 ns, which can be further increased operating with a 4 s extraction or a smaller number of pot per cycle. The occurrence of a neutrino interaction in the detector can thus be time linked with the observation of the lepton in the decay tunnel. Such an observation has never been perfomed in any neutrino experiment at any energy and would represent a major breakthrough in experimental neutrino physics. A facility where the neutrino is uniquely associated with the other decay particles of the parent kaon is called a "tagged neutrino beam". Physicists have been speculated about this possibility just after the first direct observation of neutrinos [21, 22, 23, 24, 25, 26] but the technologies that provide time resolution, pile-up mitigation and radiation hardness for time tagged neutrino beams are available since a few years only. In order to suppress accidental coincidences between the neutrino interaction and uncorrelated particles inside the beam pipe, the timing precision of the detectors that are used to instrument the decay tunnel must reach 100 ps. This precision is needed also to associate the positron with the other decay product of the kaons. The physics potential of tagged neutrino beams are enormous beacuse they provide energy and flavor measurement on event-by-event basis and are the ideal tool to study cross sections and non standard oscillation phenomena, including sterile

neutrinos. They also give experimental access to the lepton-neutrino entangled state to study propagation and collapse of the wavefunction.

ENUBET will consider tagged neutrino beams as a natural evolution of its physics programme and will study the optimal beamline configuration for these novel facilities. On the other hand, R&D on the photon tagger and the neutrino detector to bring time resolution to 100 ps requires dedicated resources. Given the potential and physics reach of tagged neutrino beams seed fundings have already been provided by the Italian Ministry for Research and Education. Applications for grants dedicated specifically on tagged neutrino beams are being submitted.

9 Requested support from CERN

In the first two years of the project, the collaboration with the CERN groups, the tests performed at the SPS and the use of the East Area beamline for the characterization of the prototypes were prominent for the success of ENUBET. The most relevant requests for 2019-2021 can be summarized as follows:

- support and consulting from CERN accelerator experts in the design of the ENUBET beamline in collaboration with personnel employed by the project
- the use of a test beamline in the Renovated East Area for the final validation of the demonstrator. For 2021, we request 5 weeks in two separate periods (2 weeks + 3 weeks).
- a test of the final proton extraction scheme of ENUBET in the SPS after LS2

In the early stage of the project, the ENUBET activities have been framed into NP03/Plafond (General R&D platform for neutrino detectors). After this preliminary phase, the tasks of the project have been detailed and the collaboration with the CERN groups fully established. We thus propose the creation of NP06/ENUBET with the aim of delivering the demonstrator of the positron tagger and the conceptual design of the ENUBET beamline by the end of 2021.

10 Conclusions

During the first two years of activities, ENUBET has achieved important milestones and extended remarkably its physics case. The R&D carried out in collaboration with CERN includes the proton extraction schemes, the design of the transfer line and the beam tests of the prototypes at the CERN East Area. The project is aimed at delivering a complete design of the ENUBET beamline by 2021 and test the demonstrator of the instrumentation of the decay tunnel just after LS2. Beyond ν_e cross section measurements, the ENUBET physics potential is being investigated for the study of

ν_μ interactions, the determination of differential cross-sections employing the narrow-band off-axis technique and for non-standard oscillation physics. The static focusing system opens up the possibility of transforming ENUBET in the world first tagged neutrino beams and the corresponding technical challenges are being addressed.

References

[1] S. E. Kopp, Phys. Rept. **439** (2007) 101

[2] T. Katori and M. Martini, J. Phys. G **45** (2018) no.1, 013001

[3] L. Alvarez-Ruso *et al.*, Prog. Part. Nucl. Phys. **100** (2018) 1

[4] A. M. Ankowski and C. Mariani, J. Phys. G **44** (2017) no.5, 054001

[5] A. Longhin, L. Ludovici and F. Terranova, Eur. Phys. J. C **75** (2015) 155.

[6] A. Berra *et al.*, CERN-SPSC-2016-036, SPSC-EOI-014, Geneva, 2014.

[7] Documentation available at `http://enubet.pd.infn.it/`

[8] H. Weisberg, Effective Spill Length Monitor, AGS devision technical note BNL-104591-2014-IR, Brookhaven National Laboratory, New York, 1980

[9] V. Kain, K. Cornelis and E. Effinger, "New Spill Control for the Slow Extraction in the Multi-Cycling SPS", Proceedings of IPAC2016, Busan, Korea

[10] D. C. Carey, K. L. Brown, F. Rothacher, SLAC-R-95-462, Stanford, 1995.

[11] T. J. Roberts, K. B. Beard, D. Huang, S. Ahmed, D. M. Kaplan and L. K. Spentzouris, Conf. Proc. C **0806233** (2008) WEPP120.

[12] F. Terranova, Talk at 39th International Conference on High Energy Physics (ICHEP2018), Seoul, Korea, 5-12 July 2018.

[13] G. Brunetti, Talk at 20th International Workshop on Neutrinos from Accelerators, Blacksburg, Virginia, August 12-18, 2018.

[14] A. Berra *et al.*, IEEE Trans. Nucl. Sci. **58** (2011) 1297.

[15] A. Berra *et al.*, proc. of 17th International Workshop on Neutrino Factories and Future Neutrino Facilities (NuFact15) : Rio de Janeiro, Brazil, arXiv:1512.08202 [hep-ex].

[16] A. Berra *et al.*, Nucl. Instrum. Meth. A **830** (2016) 345.

[17] Full list of publications available at `http://enubet.pd.infn.it/pub.html`.

[18] G. Ballerini *et al.*, JINST **13** (2018) P01028

[19] A. Coffani *et al.*, Prospects in Neutrino Physics (NuPhys2017), 20-22 Dec 2017. London, UK, arXiv:1804.03248 [physics.ins-det]. F. Acerbi *et al.*, in preparation.

[20] A. Meregaglia, Talk at 30th Rencontres de Blois, Blois, 3-8 June 2018.

[21] L. N. Hand, "A study of 40-90 GeV neutrino interactions using a tagged neutrino beam," Proceedings of Second NAL Summer Study, Aspen, Colorado, 9 Jun - 3 Aug 1969, p.37.

[22] B. Pontecorvo, Lett. Nuovo Cim. **25** (1979) 257.

[23] P. Denisov *et al.*, preprint IHEP 81-98, Serpukhov, 1981.

[24] R.H. Bernstein *et al.*, FERMILAB-Proposal-0788, 1989.

[25] L. Ludovici and P. Zucchelli, [hep-ex/9701007].

[26] L. Ludovici and F. Terranova, Eur. Phys. J. C **69** (2010) 331.